Coexistence and Coupling of Spin-Induced Ferroelectricity and Ferromagnetism in Perovskites

Junting Zhang,[1,*] Ying Zhou,[1] Fan Wang,[1] Xiaofan Shen,[1] Jianli Wang,[1] and Xiaomei Lu[2,†]
[1]School of Materials Science and Physics, China University of Mining and Technology, Xuzhou 221116, China
[2]National Laboratory of Solid State Microstructures and Physics School, Nanjing University, Nanjing 210093, China

(Received 29 August 2021; revised 3 December 2021; accepted 25 August 2022; published 9 September 2022)

Spin-induced ferroelectricity usually does not occur in perovskites with simple collinear magnetic structures. Here, we demonstrate that in even-layer perovskite systems, some common distortion modes involving octahedral rotation and Jahn-Teller distortion can break the inversion symmetry, allowing the emergence of spin-dependent out-of-plane polarization in a simple magnetic structure. Such spin-induced ferroelectricity is very common in double-perovskite systems and can coexist with ferromagnetism or ferrimagnetism above room temperature. We explain its origin by modifying the spin-dependent *p-d* hybridization mechanism. Our Letter provides a universal design for two-dimensional multiferroics and enables the control of polarization by means of a magnetic field.

DOI: 10.1103/PhysRevLett.129.117603

In crystals lacking an inversion center, spin-orbit coupling (SOC) enables a variety of fascinating phenomena, such as inducing a momentum-dependent effective magnetic field that leads to spin splitting in nonmagnetic materials [1–4]. In addition, SOC provides a strong coupling between spin and valley degrees of freedom in the monolayers of transition metal dichalcogenides [5,6]. In magnetically ordered materials, SOC may also play a key role in spin-induced ferroelectricity [7,8], namely the type-II multiferroics, which have great application prospects in the cross control of magnetoelectricity [9–12]. Generally, spin-induced ferroelectricity requires a complex antiferromagnetic order to break the spatial inversion symmetry [11,12] such as spiral spin order [13,14] or collinear ↑↑↓↓ order [15,16], which are difficult to control by magnetic field. In addition, low magnetic order temperature and weak ferroelectric polarization are still the main drawbacks facing spin-induced ferroelectricity, which limit the application in devices [17,18].

In fact, inversion symmetry breaking (ISB) can be caused by other degrees of freedom besides spin order, such as lattice, charge, and orbital orders [19–22]. From the perspective of symmetry, a single spin, acting as an axis vector under SOC [23], breaks the symmetry operation of changing the direction of spin axis, which can lead to the breaking of nonpolar point groups to polar point groups and the emergence of spin-dependent polarization (see Fig. 1). Microscopically, in the absence of inversion symmetry at the spin site, the mixing of odd-even parity via *p-d* hybridization can lead to polarized charge distributions that are related to electron orbital and therefore spin dependent through SOC [24]. Therefore, ISB caused by other degrees of freedom is a prerequisite for spin-induced ferroelectricity in a simple magnetic structure. ISB is known to occur when some bulk crystals are reduced to two dimensional (2D) [25,26]. Recently, the successful growth of the freestanding perovskite oxides down to the monolayer limit [27,28] provides a great opportunity to design 2D perovskite-based functionalities, such as 2D multiferroics with octahedral rotation-induced ferroelectricity proposed in our previous Letter [29].

In this Letter, we show the extensive spin-induced ferroelectricity and its compatibility with ferromagnetism in 2D perovskites. Unlike octahedral rotation-induced ferroelectricity, which requires a specific type of octahedral rotation to break into the polar point group and is independent of magnetism, the spin-induced ferroelectricity found in this Letter can occur in magnets lacking

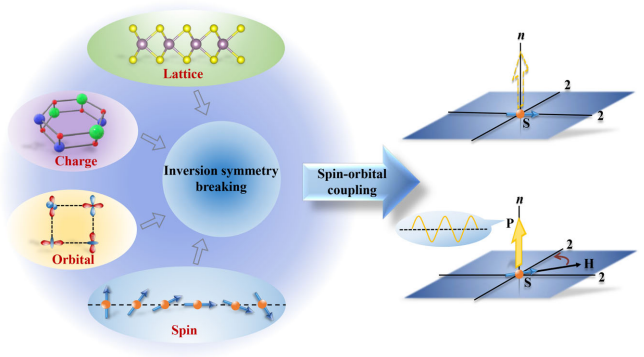

FIG. 1. Schematic of ISB caused by lattice, charge, orbital, and spin orders. In the case of ISB, a single spin (**S**) can break the nonpolar point groups (such as the D_n point group shown on the right) into the polar point groups via SOC, resulting in the emergence of spin-dependent polarization (**P**). This enables the control of polarization by magnetic field (**H**).

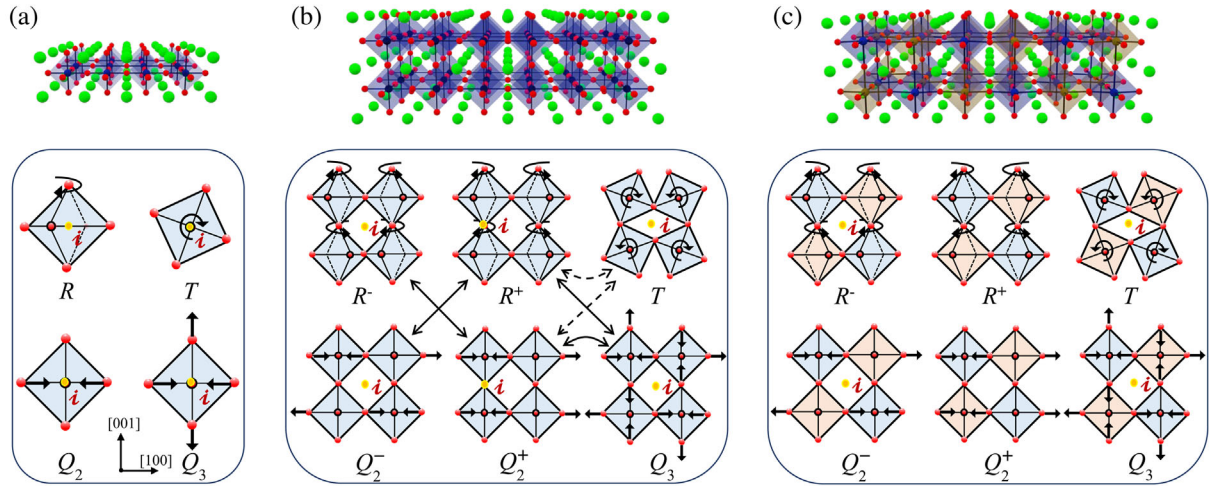

FIG. 2. Schematic octahedral rotation and JT distortion of (a) perovskite monolayer, (b) perovskite bilayer, and (c) DP bilayer with the rock-salt ordering. The solid dot marked by the letter "i" represents the inversion center existing in the distorted structure. The curved arrow around the octahedron indicates the rotation direction. The straight arrow connecting the anion represents its displacement in the JT distortion. For the perovskite bilayer, the solid and dashed double arrows indicate that the combination of the two modes leads to nonpolar and polar point groups, respectively.

inversion center and is dependent on spin direction. We demonstrate that the spin-induced out-of-plane (OP) ferroelectricity can coexist and be coupled with ferromagnetism by combining symmetry analysis and first-principles calculations (more details are given in the Supplemental Material [30]). We explain this spin-induced ferroelectricity by modifying the spin-dependent p-d hybridization mechanism.

Octahedral rotation and Jahn-Teller (JT) distortion, as the two most common types of lattice distortion in perovskites, do not break the inversion symmetry in ABX_3 perovskite bulks [39]. In the 2D perovskite, octahedral rotation distortion can be divided into rotation and tilt modes [see Fig. 2(a)]. The JT distortion of an individual BX_6 octahedron can be decomposed into Q_2 and Q_3 modes, which respectively refer to two B-X bonds elongation and two contraction (Q_2), as well as two bonds elongation and the remaining four contraction (Q_3). In the perovskite monolayer, each octahedral distortion mode retains the inversion center at the center of octahedron, which rules out the possibility of ISB caused by octahedral distortion.

When extended to the perovskite bilayer, the possible inversion center shifts to the A or X site of the perovskite prototype phase [see Fig. 2(b)]. The octahedral rotation modes can be divided into in-phase and out-of-phase rotation, denoted as R^+ and R^-, respectively. Similarly, the Q_2 mode can be divided into Q_2^+ and Q_2^- with the same sign meaning. Of all the octahedral distortion modes, the in-phase distortion modes containing R^+ and Q_2^+ take the X site as the inversion center, while the remaining modes take the A site as the inversion center [see Fig. 2(b)]. Therefore, in the perovskite bilayer, the combination of two octahedral distortion modes with different inversion centers can break the inversion symmetry. Among them, the combination of R^+ (or Q_2^+) and tilt modes directly leads to a polar point group, allowing the emergence of in-plane (IP) ferroelectricity.

Some specific combinations such as $R^+ \oplus Q_2^-$ and $R^- \oplus Q_2^+$ break the inversion symmetry into the nonpolar point groups. The coexistence of octahedral rotation and JT distortion is common in perovskites [39]. The most typical example is perovskite manganese oxides, whose crystal structure is stabilized by the octahedral rotation and the cooperative Q_2^+-type JT distortion [40]. Similar examples can also be found in perovskite fluorides, such as $NaCuF_3$ and $KCrF_3$ [39].

Cationic ordering, as a common ordering scheme of perovskites, provides an additional degree of freedom for adjusting and designing the functional properties of perovskites [41,42]. The introduction of cationic ordering can further reduce the requirement of structural distortion mode for ISB. The common cationic ordering in perovskites is the B-site order, which usually requires a large difference in the valence state and ionic radius between two types of transition-metal ions, such as the $3d$-$5d$ combination [41]. Many B-site ordered double-perovskite (DP) oxides exhibit ferromagnetism (or ferrimagnetism) with high Curie temperature [41,43]. Therefore, achieving ISB in the 2D DP system is expected to realize the coexistence of ferromagnetism and ferroelectricity above room temperature.

We first consider the most common B-site ordering configuration: the rock-salt ordering [41]. Similar to the perovskite monolayer, ISB is absent in the DP monolayer. For the DP bilayer, this cationic ordering limits the

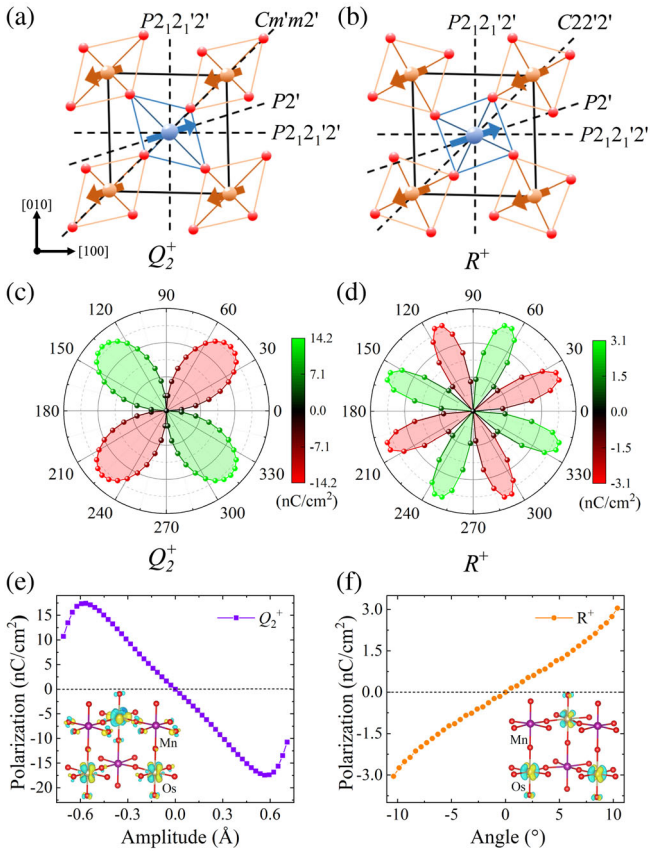

FIG. 3. Dependence of magnetic symmetry on the IP spin direction in the distorted structures caused by the (a) Q_2^+ and (b) R^+ modes individually. The arrows represent the spin of the magnetic ions. (c) and (d) show the variation of the OP polarization with the IP spin direction in the distorted structures of the Ca_3MnOsO_7 bilayer caused by a single Q_2^+ and R^+ mode, respectively. (e) Calculated polarization as a function of the amplitude of the Q_2^+ mode. The inset shows the charge density difference between the spin along the [100] and [110] directions. (f) Calculated polarization as a function of the amplitude of the R^+ mode (represented by the octahedral rotation angle). The inset shows the charge density difference between the spin along the [100] and [120] directions.

inversion center to only exist at the perovskite A site. Therefore, the inversion center is absent in the in-phase distortion modes involving R^+ and Q_2^+ modes [see Fig. 2(c)]. Similar ISB also exists in other even-layer systems, in which the symmetry of the distortion modes is independent of the number of layers (see Fig. S1 [30]). The ISB caused by octahedral distortion also occurs in the columnar ordered DP bilayer, while the layered ordering directly leads to the polar point groups (see Fig. S2 [30]).

In the DP bilayer with the rock-salt ordering, the Q_2^+ mode leads to a nonpolar $P\bar{4}2_1m$ space group. Figure 3(a) shows its magnetic symmetry depending on the IP spin direction under a simple collinear magnetic structure. Note that the ferromagnetic and A-, C-, G-type antiferromagnetic orders have the same magnetic symmetry. When the spin direction changes from [100] to [110], the magnetic space group undergoes transitions as $P2_12_1'2' \rightarrow P2' \rightarrow Cm'm2'$. That is, the IP spin orientation other than the [100] equivalent direction breaks the IP twofold screw axes (2_1) while retaining the OP twofold rotation axis ($2'$), thus allowing the emergence of the OP polarization. Similarly, for the distorted structure ($P42_12$) caused by the R^+ mode, the magnetic symmetry is the same as that of the Q_2^+ modes, except that the [110] spin direction retains the IP twofold rotation axes ($C22'2'$) and thus causes the polarization to disappear [see Fig. 3(b)].

This spin-dependent polarization was confirmed by first-principles calculations. In the distorted structure caused by the Q_2^+ mode, the spin-induced polarization disappears in the [100] equivalent direction [see Fig. 3(c)], consistent with the symmetry analysis above. Polarization reaches its maximum when the spin is along the [110] equivalent direction, and changes sign as the spin is rotated 90° in the plane. In contrast, for the distorted structure caused by the R^+ mode, the polarization curve shows fourfold symmetry [see Fig. 3(d)]. The polarization disappears when the spin is along the equivalent direction of [100] and [110], and reaches its maximum when the spin is along their middle direction. The spin-induced polarization is proportional to the amplitude of the corresponding mode, and reverses its direction as the mode sign changes [see Figs. 3(e) and 3(f)]. However, for the Ca_3MnOsO_7 bilayer, when the amplitude of the Q_2^+ mode exceeds a certain value, the change of polarization with amplitude shows an opposite trend, which may be related to the transition of the electronic configuration of the $5d$ ion (see Fig. S3) [30,44].

This spin-induced polarization and its dependence on the spin direction can be explained by modifying the spin-dependent p-d hybridization mechanism. According to previous research [24,45], the ionic charges of magnetic ions and ligands vary with the spin direction due to the modification of p-d hybridization by SOC. The modification of the charge transfer can be described as $\Delta\rho \propto (\mathbf{S}\cdot\mathbf{e})^2$, where $\mathbf{e}$ is the unit vector along the bond connecting the magnetic ion and the ligand. However, this formula cannot directly explain the spin-dependent OP polarization demonstrated above, because the p-d hybridization of the OP bonds does not change with the IP spin direction according to this formula. In fact, in an individual octahedron, the p-d hybridization of the OP bonds is influenced by that of the IP bonds, since some d orbitals (such as d_{xz}/d_{yz} orbitals) are involved in the formation of both IP and OP covalent bonds. The charge transfer along the IP bonds changes the charge of the magnetic ion, resulting in a change in the p-d hybridization of the OP bonds. Because of the difference in the coordination of the top and bottom anions in an octahedron, the covalence and charge transfer of the two vertical bonds is different, resulting in an OP electric dipole moment in each octahedron. This local electric dipole moment depends on the IP

spin direction according to the above analysis. If the spin is along the general direction, the local electric dipole moment of the octahedrons in the upper and lower layers is not cancelled, resulting in a net OP polarization.

The differential charge density [the insets of Figs. 3(e) and 3(f)] shows that the charge transfer caused by the change of spin direction is mainly concentrated on the $5d$ ion, due to its strong SOC effect. The charge redistribution of the O ions in the surface layer is more significant than that of the O ions in the middle layer. For the distorted structure caused by the Q_2^+ mode, when the spin is in a direction other than [100] equivalent direction, the longest bonds of the same magnetic ions in the upper and lower layers have different angles to the spin direction, resulting in different orbital component and ionic charge (see Fig. S4 [30]). This is also reflected in the difference in magnetic moment of $5d$ ions between the upper and lower layers, which varies with the spin direction (see Fig. S5 [30]). The spin-dependent polarization in this distorted structure can be expressed as [30]

$$P_{Q_2^+} \propto \sin 2\theta, \tag{1}$$

where θ is the angle between the spin and the [100] direction.

For the distorted structure caused by the R^+ mode, the charge transfer from the IP ligands to the magnetic ion in an octahedron cancels out according to the formula $\Delta\rho \propto (\mathbf{S}\cdot\mathbf{e})^2$, which therefore cannot explain the spin-dependent polarization. In fact, this formula is derived from the lowest-order perturbation of SOC to p-d hybridization [45]. The higher-order perturbation terms may be considerable due to the strong SOC of the $5d$ ions, and can play an important role when the effect of the lowest-order perturbation disappears. Considering the second-order perturbation effect, the modification of the charge transfer between the magnetic ion and its ligand can be described as $\Delta\rho^{(2)} \propto (\mathbf{S}\cdot\mathbf{e})^4$. According to this expression, the spin-dependent polarization can be derived as [30]

$$P_{R^+} \propto \sin 4\theta \sin 4\varphi, \tag{2}$$

where φ is the rotation angle of the octahedron. The dependence of polarization on the spin direction and octahedral rotation angle is well explained by this expression.

Next, we determine the ground-state structures of some selected materials to calculate the actual spin-induced polarization. For comparison, we select some different combinations of $3d$ and $5d$ ions, including JT-active Mn^{3+} and nonactive Fe^{3+} for $3d$ ions, and $5d$ ions with half-full (Os^{5+}) and partially occupied (Re^{5+} or Re^{6+}) t_{2g} orbital. We analyze the symmetry with different cation orderings and various octahedral distortion, and calculate the energy of each structural phase (Tables S1 and S2 [30]).

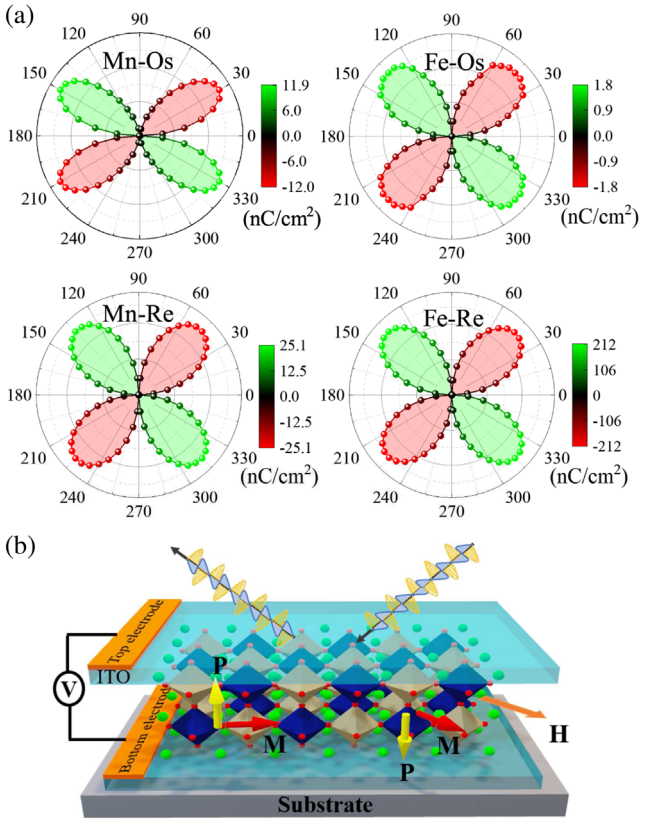

FIG. 4. (a) Dependence of the OP polarization on the IP spin direction in the ground-state phases of the four Ca-based bilayers. (b) Schematic of the application prototype of the coupling between spin-induced polarization (**P**) and magnetization (**M**).

These DP bilayers tend to form rock-salt ordering, and the antisite disorder constructed in special quasirandom structures has obviously higher energy, similar to their bulk phases [41,46]. Their ground-state phases have the $P2_1$ symmetry with $a^-a^-c^+$ octahedral rotation, which is compatible with the Q_2^+ mode. Phono spectra and first-principles molecular dynamics simulation (at 300 K) confirm their dynamic and thermal stability, respectively (see Fig. S6 [30]). Their ground-state phases (except Mn-Re bilayer) exhibit a G-type antiferromagnetic order (Table S3 [30]), which results in ferrimagnetism due to the difference in magnetic moments of $3d$ and $5d$ ions. Magnetic anisotropy calculations show that the easy-magnetization axes of these ferrimagnetic and antiferromagnetic (Mn-Re) bilayers lie perpendicular and parallel to the tilt axis, respectively (see Fig. S7 [30]). Monte Carlo simulation further confirms the magnetic ground states and estimates the magnetic transition temperature (see Fig. S8 [30]). Among these bilayers, the Curie temperature (470 K) of the Fe-Re bilayer is far above room temperature.

Figure 4(a) shows the calculated spin-dependent OP polarization of these bilayers. The distribution of polarization with the IP spin direction is symmetric about the [100] and [010] directions, which is determined by the only

crystal symmetry operation 2_1 [30]. Although the charge transfer caused by SOC is mainly concentrated on the 5*d* ions, the induced polarization strongly depends on the combined 3*d* ions. For example, the maximum polarization of the Fe-Os bilayer is much smaller than that of the Mn-Os bilayer, which may be related to its larger energy level difference between the occupied and unoccupied t_{2g} orbitals of the Os ion (see Fig. S9 [30]). In contrast, the maximum polarization of the Fe-Re bilayer is much greater than that of the Mn-Re bilayer, which can be attributed to the transition of the occupied *d* orbital of Re ion, i.e., from d_{xy}/d_{xz} (or d_{xy}/d_{yz}) in the former (Fe^{3+}-Re^{5+}) to d_{xy} in the latter (Mn^{2+}-Re^{6+}). The maximum polarization (212 nC/cm^2) of the Fe-Re bilayer has reached the magnitude of the polarization induced by the exchange-striction mechanism [11,17]. The coupling coefficients (Table S4 [30]) can be evaluated from the polarization curves. While similar spin-dependent polarization exists in other even-layer systems, the induced polarization is significantly reduced with respect to the bilayer system, although the distortion modes are essentially unchanged (see Fig. S10 and Table S5 [30]). This may be due to the fact that the spin-induced polarization depends on the difference between the O ion charge at the top and bottom of a single octahedron, which is particularly significant in the surface perovskite layer.

Both octahedral rotation-induced IP ferroelectricity and spin-induced OP ferroelectricity can occur when the R^+ and tilt modes coexist, such as the ground-state structure of the selected four bilayers (Table S4 [30]). Note that although their magnetic ground states are ferrimagnetic or antiferromagnetic, such spin-induced ferroelectricity is also present in the ferromagnetic order due to the same magnetic symmetry. Furthermore, similar spin-induced ferroelectricity can occur in other 2D ferromagnets lacking inversion symmetry besides perovskites (see Fig. S11 [30]). The coexistence and coupling between spin-induced polarization and magnetization enables the control of polarization by magnetic field, providing potential applications in devices [see Fig. 4(b)], such as electromagnon excitation and directional dichroism [23,47,48]. Note, however, that the polarization value is still much smaller than that of conventional perovskite ferroelectrics, and therefore the order of magnitude of spin-induced polarization needs to be further improved before its practical application for microelectronics.

In conclusion, we demonstrate the extensive spin-induced ferroelectricity and its coexistence and coupling with ferromagnetism or ferrimagnetism in even-layer DP systems. This ferroelectricity can be explained by a modified *p-d* hybridization mechanism in which SOC causes differences in *p-d* hybridization and charge transfer between adjacent perovskite layers, resulting in spin-direction-dependent OP polarization. By designing the combination of magnetic ions, not only can the coexistence of ferroelectricity and ferromagnetism above room temperature be achieved, but also the spin-induced polarization can be significantly improved. This Letter provides a new perspective for realizing 2D multiferroics and magnetoelectric cross control.

We thank Shuai Dong for helpful discussions. This work was financially supported by the National Natural Science Foundation of China (Grants No. 11974418, 51721001, and 11874208), and the Fundamental Research Funds for the Central Universities (Grant No. 2019QNA30). Computer resources provided by the High Performance Computing Center of Nanjing University are gratefully acknowledged.

*Corresponding author.
juntingzhang@cumt.edu.cn
†Corresponding author.
xiaomeil@nju.edu.cn

[1] G. Dresselhaus, Phys. Rev. **100**, 580 (1955).
[2] E. Rashba, Sov. Phys. Solid State **2**, 1109 (1960).
[3] K.-W. Kim, H.-W. Lee, K.-J. Lee, and M. D. Stiles, Phys. Rev. Lett. **111**, 216601 (2013).
[4] A. Manchon, H. C. Koo, J. Nitta, S. M. Frolov, and R. A. Duine, Nat. Mater. **14**, 871 (2015).
[5] W.-Y. Tong, S.-J. Gong, X. Wan, and C.-G. Duan, Nat. Commun. **7**, 13612 (2016).
[6] J. R. Schaibley, H. Yu, G. Clark, P. Rivera, J. S. Ross, K. L. Seyler, W. Yao, and X. Xu, Nat. Rev. Mater. **1**, 16055 (2016).
[7] H. Katsura, N. Nagaosa, and A. V. Balatsky, Phys. Rev. Lett. **95**, 057205 (2005).
[8] H. J. Xiang, E. J. Kan, Y. Zhang, M.-H. Whangbo, and X. G. Gong, Phys. Rev. Lett. **107**, 157202 (2011).
[9] T. Kimura, T. Goto, H. Shintani, K. Ishizaka, T. Arima, and Y. Tokura, Nature (London) **426**, 55 (2003).
[10] Y. Kitagawa, Y. Hiraoka, T. Honda, T. Ishikura, H. Nakamura, and T. Kimura, Nat. Mater. **9**, 797 (2010).
[11] Y. Tokura, S. Seki, and N. Nagaosa, Rep. Prog. Phys. **77**, 076501 (2014).
[12] N. A. Spaldin and R. Ramesh, Nat. Mater. **18**, 203 (2019).
[13] X. Rocquefelte, K. Schwarz, P. Blaha, S. Kumarand, and J. vanden Brink, Nat. Commun. **4**, 2511 (2013).
[14] E. Bousquet and A. Cano, J. Phys. Condens. Matter **28**, 123001 (2016).
[15] I. A. Sergienko, C. Sen, and E. Dagotto, Phys. Rev. Lett. **97**, 227204 (2006).
[16] Y. J. Choi, H. T. Yi, S. Lee, Q. Huang, V. Kiryukhin, and S.-W. Cheong, Phys. Rev. Lett. **100**, 047601 (2008).
[17] S. Dong, J.-M. Liu, S.-W. Cheong, and Z. F. Ren, Adv. Phys. **64**, 519 (2015).
[18] J. T. Zhang, X. M. Lu, X. Q. Yang, J. L. Wang, and J. S. Zhu, Phys. Rev. B **93**, 075140 (2016).
[19] N. A. Benedek and C. J. Fennie, Phys. Rev. Lett. **106**, 107204 (2011).
[20] J. M. Rondinelli and C. J. Fennie, Adv. Mater. **24**, 1961 (2012).

[21] K. Singh, C. Simon, E. Cannuccia, M.-B. Lepetit, B. Corraze, E. Janod, and L. Cario, Phys. Rev. Lett. **113**, 137602 (2014).
[22] M. Fiebig, T. Lottermoser, D. Meier, and M. Trassin, Nat. Rev. Mater. **1**, 16046 (2016).
[23] M. Matsumoto, K. Chimata, and M. Koga, J. Phys. Soc. Jpn. **86**, 034704 (2017).
[24] H. Murakawa, Y. Onose, S. Miyahara, N. Furukawa, and Y. Tokura, Phys. Rev. Lett. **105**, 137202 (2010).
[25] D. Xiao, G.-B. Liu, W. Feng, X. Xu, and W. Yao, Phys. Rev. Lett. **108**, 196802 (2012).
[26] J. Lu, W. Luo, J. Feng, and H. Xiang, Nano Lett. **18**, 595 (2018).
[27] D. Lu, D. T. Baek, S. S. Hong, L. F. Kourkoutis, Y. Hikita, and H. Y. Hwang, Nat. Mater. **15**, 1255 (2016).
[28] D. X. Ji, S. H. Cai, T. R. Paudel, H. Y. Sun, C. C. Zhang, L. Han, Y. F. Wei, Y. P. Zang, M. Gu, Y. Zhang *et al.*, Nature (London) **570**, 87 (2019).
[29] J. T. Zhang, X. F. Shen, Y. C. Wang, C. Ji, Y. Zhou, J. L. Wang, F. Z. Huang, and X. M. Lu, Phys. Rev. Lett. **125**, 017601 (2020).
[30] See Supplemental Material at http://link.aps.org/supplemental/10.1103/PhysRevLett.129.117603 for computational details, derivation of the expression of spin-induced polarization, symmetry analysis of double perovskite with different cation orderings and layer numbers, energy of structural and magnetic phases, projected band structures, variation of orbital components and magnetic moment with spin direction, molecular dynamics simulation and phonon spectra, magnetic anisotropy, magnetic exchange interactions and Monte Carlo simulation, polarization components and coupling coefficients, spin-dependent polarization and the amplitude of distortion modes of different even layers, and spin-dependent polarization of $2H$-VSe_2 monolayer, which includes Refs. [31–38].
[31] P. E. Blöchl, Phys. Rev. B **50**, 17953 (1994).
[32] G. Kresse and J. Furthmüller, Phys. Rev. B **54**, 11169 (1996).
[33] J. P. Perdew, A. Ruzsinszky, G. I. Csonka, O. A. Vydrov, G. E. Scuseria, L. A. Constantin, X. L. Zhou, and K. Burke, Phys. Rev. Lett. **100**, 136406 (2008).
[34] S. L. Dudarev, G. A. Botton, S. Y. Savrasov, C. J. Humphreys, and A. P. Sutton, Phys. Rev. B **57**, 1505 (1998).
[35] X. F. Shen, Q. Y. Luo, Z. S. Wu, Y. Zhou, J. L. Wang, J. T. Zhang, J. Su, and X. M. Lu, Phys. Rev. B **103**, L220406 (2021).
[36] R. D. King-Smith and D. Vanderbilt, Phys. Rev. B **47**, 1651 (1993).
[37] B. J. Campbell, H. T. Stokes, D. E. Tanner, and D. M. Hatch, J. Appl. Crystallogr. **39**, 607 (2006).
[38] A. Togo and I. Tanaka, Scr. Mater. **108**, 1 (2015).
[39] M. A. Carpenter and C. J. Howard, Acta Crystallogr. Sect. B **65**, 134 (2009).
[40] T. Kimura, S. Ishihara, H. Shintani, T. Arima, K. T. Takahashi, K. Ishizaka, and Y. Tokura, Phys. Rev. B **68**, 060403(R) (2003).
[41] S. Vasala and M. Karppinen, Prog. Solid State Chem. **43**, 1 (2015).
[42] M. W. Lufaso and P. M. Woodward, Acta Crystallogr. Sect. B **60**, 10 (2004).
[43] D. Serrate, J. M. D. Teresa, and M. R. Ibarra, J. Phys. Condens. Matter **19**, 023201 (2007).
[44] I. Solovyev, N. Hamada, and K. Terakura, Phys. Rev. Lett. **76**, 4825 (1996).
[45] C. Jia, S. Onoda, N. Nagaosa, and J. H. Han, Phys. Rev. B **74**, 224444 (2006).
[46] M. Shaikh, A. Fathima, M. J. Swamynadhan, H. Das, and S. Ghosh, Chem. Mater. **33**, 1594 (2021).
[47] Y. Takahashi, R. Shimano, Y. Kaneko, H. Murakawa, and Y. Tokura, Nat. Phys. **8**, 121 (2012).
[48] J. M. Hu, T. X. Nan, N. X. Sun, and L. Q. Chen, MRS Bull. **40**, 728 (2015).